11th IGTC
Dispatchable technology & innovations for a carbon-neutral society
10-11 October 2023, Brussels, Belgium
Paper ID Number: 12-IGTC23

THE POTENTIAL OF sCO_2 CYCLES AS BOTTOMING CYCLE FOR GAS TURBINES

Vincent THIELENS, Thermal Engineering and Combustion Unit, University of Mons (UMONS)
Frederiek DEMEYER, Mechanics and Thermal processes, ENGIE R&I (Laborelec)
Ward DE PAEPE, Thermal Engineering and Combustion Unit, University of Mons (UMONS)

Place du Parc 20, 7000 MONS, Belgium
+32 (0)491 63 28 19
vincent.thielens@umons.ac.be

KEYWORDS
sCO_2 cycles, performance maps, techno-economic assessment, bottoming cycles, carbon capture

ABSTRACT
Gas turbines are a popular technology for coping with the intermittency of renewables due to their fast start-up time, inherent flexibility and large part load efficiency. Moreover, the high turbine outlet temperature leads to a significant valorisation opportunity. While adding a bottoming cycle increases the fuel efficiency up to 60%, the high capital costs of steam technologies make them less attractive for smaller GT units. Nevertheless, the use of sCO_2 as working fluid can simplify installations and potentially provide a more affordable solution. This article explores the potential of waste heat recovery for power generation using sCO_2 cycles. Different sCO_2 cycles are presented with their advantages and limitations, and performance maps have been created to link the waste heat stream temperature to their performances. The article shows that the performances of sCO_2 can outperform steam and LCOE for different scales of GTs. Furthermore, a comparison between an SGT5 9000HL coupled with a three-pressure steam cycle, and a sCO_2 cycle has been performed to understand the differences between the two bottoming technologies. As cogeneration is an interesting option for supercritical cycles, the integration of an amine-based carbon capture with heat requirements for the stripper has been investigated.

INTRODUCTION

Recent years have seen an evolution in interest on the topic of sCO_2 technologies as evidences the tremendous increase in the number of documents and patents related to sCO_2 (White et al., 2021). Indeed, supercritical cycles present some advantages over the traditional steam power cycles. This can be illustrated by the higher thermal efficiency, due to the higher fluid density and the specific heat capacity of sCO_2, as the absence of a phase change (Liu et al., 2019). Furthermore, the high density of sCO_2 also leads to compact installations that significantly reduce the turbomachinery (Brun et al., 2017), and potentially the cost when an economy of scale will be established. Looking at the other alternatives to steam cycles like the ORCs, CO_2 has a lower GWP than many organic fluids and is non-flammable. Besides, the simplicity in the configuration of supercritical cycles enhances flexible operation allowing the cycle to be operated at variable load and to be started/stopped quickly and more frequently (Cagnac et al., 2019). These characteristics offer a strong advantage to balance the intermittent input from renewable energy sources on the grid.

In the framework of bottoming cycles, some articles have already described the impact of the exhaust gas temperature on the cycle performance (Cagnac et al., 2019; Stepanek et al., 2020). However, the majority of the publications only presents the performances achievable for given conditions, while the use of the exergy concept is not frequent (Crespi et al., 2017). In this article, the focus is firstly on the assessment of performance maps that allow to quickly evaluate the performances of a cycle for a given exhaust gas temperature. This provides a better view on the applicability and potential of supercritical cycles for waste heat recovery,

Table 1: Thermodynamical characteristics of the components (Alfani et al., 2021; Baggiani et al., 2022; Biondi, 2020)

Item	Value	Unit
compressor isentropic efficiency	80	%
turbine isentropic efficiency	85	%
recuperator temperature pinch	10	°C
heater temperature pinch	30	°C
cooler outlet temperature	33	°C
configuration of the exchangers	counterflow	-
minimal pressure	85	bar
maximal pressure	280	bar

and more particularly as a bottoming cycles for the current gas turbine market. Based on the data of different gas turbine manufacturers, the additional amount of power that can be produced by the addition of a sCO_2 bottoming cycle is assessed. Moreover, the costs of some main components are also included to better assess the impact on CAPEX. The computations of LCOE answer the need in industry to have trends on the cost of such installations for bottoming cycle applications on gas turbines up to 250 MWe. Whereas steam performances are said hardly beatable (Wright et al., 2016), the difference between the two technologies is here qualified to show why sCO_2 is not relevant at that scale. Based on an H-Class CCGT, an integrated approach for a sCO_2 bottoming cycle as a setup with an amine-based PCC system has been studied. Indeed, finding innovative ways to reduce the energy penalty from a PCC system is a clear demand from industry in order to achieve the CO_2 emission reduction goals set by governments (Rubin et al., 2012).

NOMENCLATURE

Acronym	Definition
a	Fit coefficient
b	Fit coefficient
C	Component cost
CC	Carbon Capture
CCGT	Combined Cycle Gas Turbine
CEPCI	Chemical Engineering Plant Cost Index
EGR	Exhaust Gas Recirculation
EoS	Equation of State
f_T	Temperature correction factor
GT	Gas Turbine
GWP	Global Warming Potential
Hirn cycle	Rankine cycle with superheating
HP	Heat Pump
HRSG	Heat Recovery Steam Generator
LMTD	Logarithm Mean Temperature Difference
$\dot{m}$	Mass flow rate
MVR	Mechanical Vapor Recompression
P	Power
PCC	Post Combustion Capture
Q	Heat
ORC	Organic Rankine cycle
ROI	Return On Investment
sCO_2	Supercritical Carbon Dioxide
SP	Scaling Parameter
T	Temperature

PERFORMANCE MAPS

There is a strong need from the industry to know when and where the application of a sCO_2 cycle is valuable. Different sCO_2 cycles exist, however each configuration results in different performances within the same range of source temperatures. Hence, to give the reader more insight in the cycle performances, different cycles used for waste heat recovery are simulated over a wide range of exhaust gas temperatures (200-800 °C) under standardized conditions (i.e., same gas composition and efficiencies of the components for the entire thermal range). The use of Aspen Plus® allowed to create performance maps as presented in figure 4.

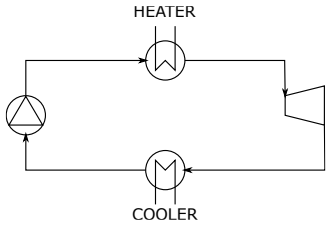

Figure 1: The simple Hirn steam cycle is used as reference to compare the performances of the supercritical cycles

A wide selection of sCO_2 cycles have been designed to suit different applications (e.g. thermal flux sources like nuclear, and waste thermal sources within waste heat recovery applications) (Crespi et al., 2017). A strong distinction between those two kinds of thermal source streams is necessary. Indeed, for a thermal flux source only the optimisation of the cycle effectiveness is mandatory; while for waste thermal streams, both the degree of source depletion as the cycle effectiveness must be maximised to achieve the highest power. The performances of the different cycle configurations, represented in figure 2, are difficult to assess since most of the components employed in sCO_2 cycles are still under development (and may fall under confidentiality policies). Nevertheless literature (Alfani et al., 2021; Baggiani et al., 2022; Biondi, 2020) provides some equipment efficiencies that are presented in table 1. Whereas these values are assumed as technologically feasible, further industrial developments will certainly refine the available data and increase the efficiency of the components in the upcoming years. Furthermore, for each selected cycle, and within a wide spectrum of exhaust flue gas temperatures (200–800 °C), the parameters maximizing the power production have been computed. Under those conditions, different equations are stated that present the net power output P_{net} per fume flow rate $\dot{m}_{exhaust\ gas}$ (eq. -1), the energy efficiency η (eq. -2), the exergy efficiency ψ_{25} (eq. -3) and specific power p_{spec} (eq. -4). The exergy j_{25} is computed with an ambient temperature of 25 °C and a pressure of 1 bar (Dincer and Rosen, 2012).

Table 2: Composition of gas turbine exhaust fed with methane and atmospheric air in excess of 1.18

Components		% vol
Nitrogen	N_2	73.7
Oxygen	O_2	10.5
Carbon dioxide	CO_2	4.7
Water	H_2O	10.2
Argon	Ar	0.9

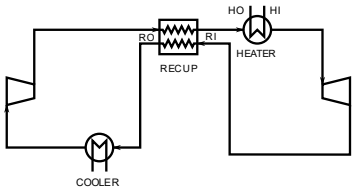

Simple Recuperative Brayton Cycle

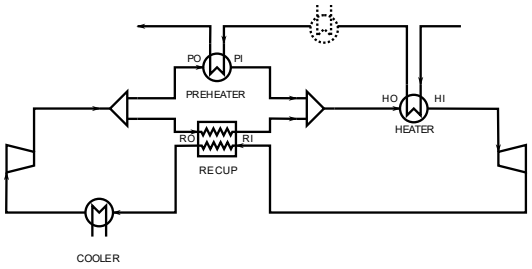

Preheating Cycle

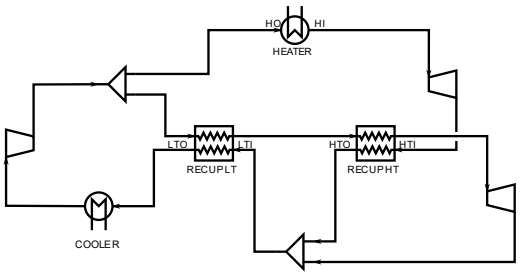

Single Heated Cascade Cycle

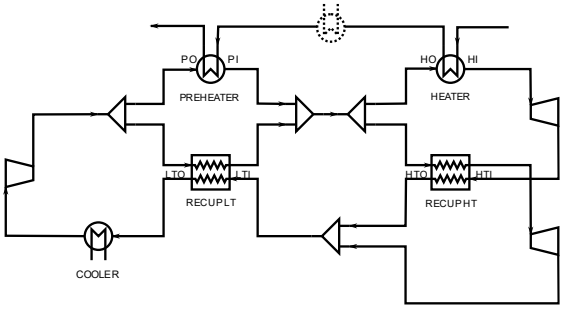

Dual Heated and Split Cascade Cycle

Figure 2: Four supercritical cycles have been chosen from (Crespi et al., 2017), and are specially suitable for WHR, the exchangers in dots referred to the part about the integration of amine-based CC

$$p_{net} = \frac{P_{net}}{\dot{m}_{exhaust\ gas}} \quad (1)$$

$$\eta = \frac{P_{net}}{Q} \quad (2)$$

$$\psi_{25} = \frac{P_{net}}{j_{25}} \quad (3)$$

$$p_{spec} = \frac{P_{net}}{\dot{m}_{sCO_2}} \quad (4)$$

Specific attention was given to the used property methods. Indeed, the properties of carbon dioxide highly fluctuate around its critical point (31.0 °C and 73.8 bar) (Brun et al., 2017). Inaccuracies in the equation of state (EoS) will therefore lead to inadequate results, especially for components working near the critical region (e.g., compressor inlet, low temperature recuperator). Amongst the equation of states, the Span-Wagner's model is the most accurate method for processes employing pure CO_2 (Span and Wagner, 1996; White and Weiland, 2018). Indeed, the Span and Wagner's EoS covers a range of temperatures between -57 °C and 826 °C, and pressures between near 0 bar and 8000 bar. The working area here considered commonly remains under 300 bar and 530 °C. The uncertainties predicted for this application range do not exceed 0.1% for density and 2% for isobaric heat capacities (Span and Wagner, 1996). The range of conditions covered is satisfying for power cycle applications. Refprop, that integrates the Span-Wagner's EoS (Lemmon et al., 2018; White and Weiland, 2018; Zhao et al., 2016), is therefore employed for all the simulations within Aspen Plus®.

The standard energy source used, consists of the exhaust gas resulting from the combustion of methane with an air excess of 1.18. The composition of the flue gas is given in the table 2. Among all the cycles presented (Crespi et al., 2017), only four of them seems valuable to be analysed on the basis of a favourable performance to complexity ratio:

1. the simple recuperative Brayton cycle - cycle 1 in (Crespi et al., 2017)
2. the preheating cycle - cycle 13 in (Crespi et al., 2017)
3. the single heated cascade cycle - cycle 20 in (Crespi et al., 2017);
4. the dual heated and split cascade cycle - cycle 27 in (Crespi et al., 2017).

Reference steam cycle

The simple Hirn cycle (figure 1) is used as reference to compare the performance of the supercritical cycles. The choice of steam instead of organic fluids is motivated by the temperature range analysed. While ORCs also present interesting performances, their narrow working conditions (150-350 °C) do not make them relevant for the realization of performance maps. The simple Hirn cycle is here chosen to dispose of a baseline, the comparison with more advanced steam configurations is deeper investigated in the following sections. The setup chosen is composed of a pump, a heater, a turbine and a cooler. The low pressure is fixed at 60 mbar and the pinch in the heater is set at 30 °C. Regarding the technological constraints, a minimum vapour fraction of 0.9 is guaranteed at the turbine outlet and an isentropic efficiency of 85% is assigned for the expansion in the turbine. To maximise the power production, two remaining degrees of freedom have been altered, being respectively the

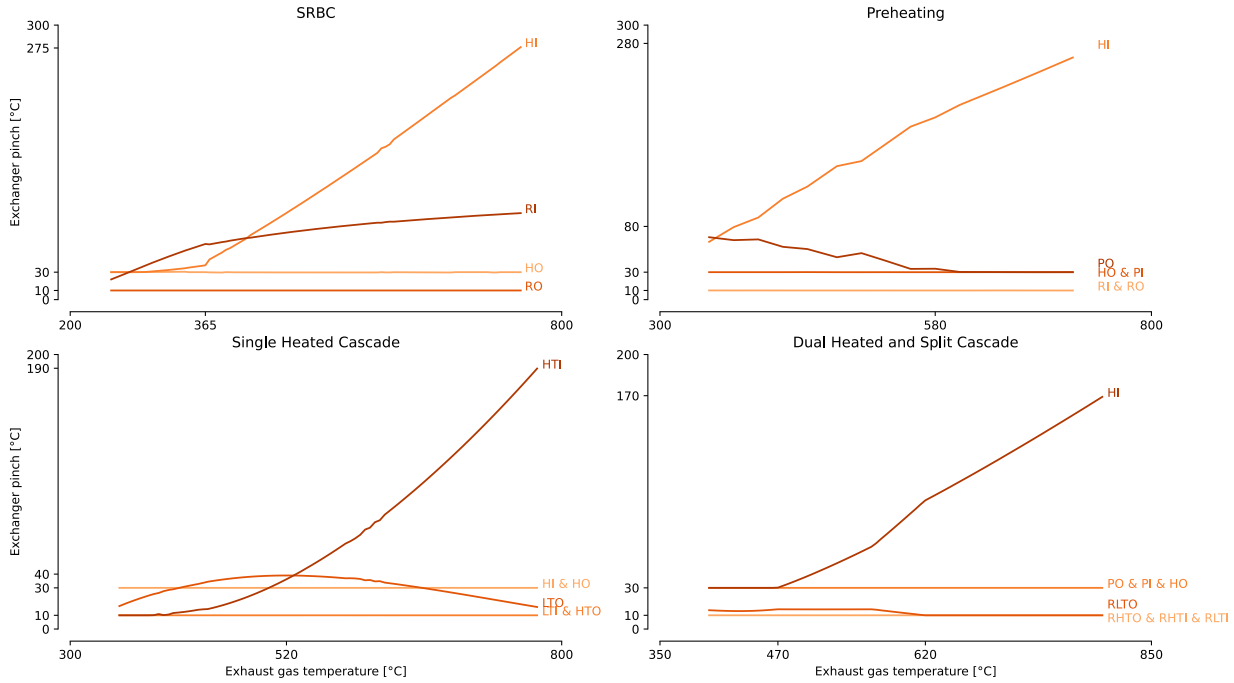

Figure 3: The pinch analysis allows to understand for the four cycles how to optimise the performances

high pressure (between 30 bar and 50 bar) and the turbine inlet temperature.

Simple recuperative Brayton - 1

The SRBC (Simple Recuperative Brayton Cycle) (figure 2a) is the most basic cycle configuration and is particularly effective for flux sources (i.e. when an amount of heat is available between two operational temperature limits); the more advanced RCBC (Recompression Closed Brayton cycle) is a proper alternative for thermal flux sources though has not been studied in the article as the focus is on waste thermal stream sources (Crespi et al., 2017). The low number of components for the SRBC makes it a reasonable low cost configuration (Cho et al., 2015). The cycle pressure ratio of 3.3 is far smaller than in steam cycles. Therefore, the carbon dioxide leaves the turbine still with a significant energetic content (Ahn et al., 2015). Consequently, adding a recuperator will increase the cycle efficiency. The maximal power production is reached when the pinch is at the hot outlet side of the exchangers (HO and RO in figure 3a) as this maximises the amount of heat recuperated in the cycle. On the first hand, the minimal pinch in the heater (HO) ensures that the exhaust gases are cooled down as low as possible, to allow a maximal energy recuperation in the cycle; on the other hand, the minimal pinch in the recuperator RO allows to recover internally as much heat as possible. By doing so, less energy is rejected to the environment through the cooler.

Preheating cycle - 13

In the preheating cycle (figure 2b), the flow is split in two after the compressor. The first substream goes through the preheater while the second one goes through the recuperator. The two flows are then mixed and follow the same process as in the SRBC. The preheater allows to increase the degree of recuperation within the cycle by cooling down the exhaust gases a bit further than in the SRBC. Having the cold, high pressure sCO_2 stream divided into two substreams helps to cope with the difference in specific heat capacity between cold high pressure and the hot low pressure sCO_2 flows. As a result, this cycle will achieve a high net power output for a small number of components. To optimise the power production, the flow rates in the two substreams should ensure that the temperature differences at both sides of the recuperator (RO and RI) are minimised (figure 3b); by doing so the exergy destruction in the recuperator is minimized.

Single heated cascade cycle - 20

The single heated cascade cycle (figure 2c) has two recuperators and two turbines. After the compressor, the flow is divided into two subcycles, one operating at a high temperature and the other at a lower temperature. After the heater, the first substream is expanded over the high temperature turbine while the remaining heat is recuperated by the second substream. The cycle produces less power and requires much more components than the preheating cycle. To optimize the power production, the temperature differences between the hot and the cold fluid must be minimized at both sides of the heater (HI and HO at figure 3c). As for the preheating cycle, it ensures that the hot exhaust gas reaches the minimal temperature, implying that the maximal amount of heat from the source is recovered. Furthermore, the hotter the working fluid after the heater, the hotter it is after the turbine. This allows to rise the

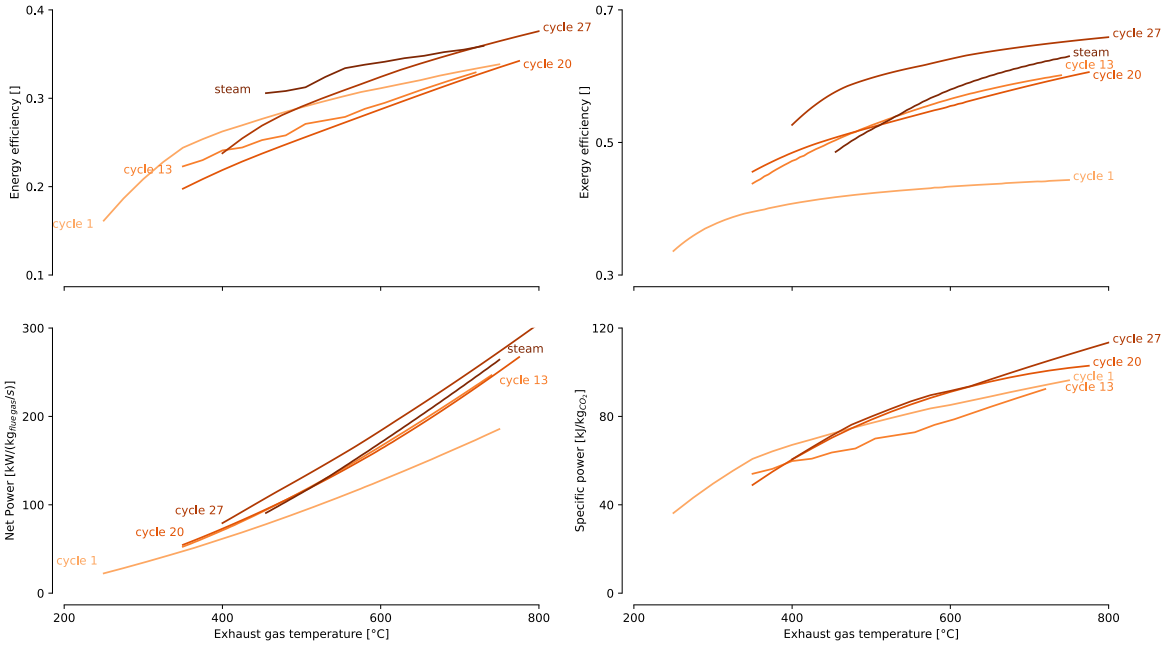

Figure 4: The performance maps show that steam power production is hardly beatable, however, sCO_2 cycles improve the potential of recuperation by a fatal heat of higher quality

temperature of the second substream in the HT recuperator, leading to a more significant global power production.

Dual heated and split cascade cycle - 27

The dual heated and split cascade cycle (figure 2d) splits the flow after the compressor. While a fraction goes through the preheater, a second stream is heated through a low temperature recuperator. The two flows are then merged and split again. The first split flow is heated in the heater before being expanded over a turbine, and its remaining heat is then recovered by the second split flow through a high temperature recuperator. This second flow is then expanded in the second turbine before being mixed again with the heater flow coming from the HT recuperator. Those two flows both travel to the hot side of the LT recuperator, and are then cooled down. The additional split in this cycle adds a degree of freedom, allowing to better optimize the cycle performances. The power production is maximised when the temperature differences respect the conditions presented in figure 3. Indeed, the HT recuperator and the preheater have to ensure minimal temperature differences for all streams at both sides of the heat exchanger (PO, PI, RHTO and RHTI). The heater hot outlet (HO) and LT recuperator hot inlet (RLTI) have also to ensure a minimal temperature difference while HI and RLTO are adapted to maximize the power production.

Comparisons of the cycles

The performances of the selected cycles are compared using performance maps. Those maps give a quick overview of the performances that a cycle can reach for a given exhaust gas inlet temperature (figure 4). At first sight, the power produced by sCO_2 cycles (figure 4c) is within the same range as the steam reference cycle. The map on exergy efficiency reports the power production to the exergy of the exhaust gases, and points at the fact that cycle 1 has a lower power production compared to the other cycle configurations. Nevertheless, the energy efficiency provided, considering the low number of components required, makes it an interesting solution for thermal flux sources. The cycle 27 comes out as the best performing cycle, however this cycle configuration requires more components. The cycles 13 and 20 present characteristics similar to the steam reference but are slightly better below 500 °C.

Energetic and exergetic efficiencies (figure 4a and 4b) are used in a different working frame. In the case of a heat flux source, i.e., an amount of energy that is given without the need to fully deploy the source (e.g., nuclear, solar), the power production is directly proportional to the energy efficiency of the cycle. The higher the energetic efficiency, the more power that can be produced. Per contra, the exergy efficiency has to be used for waste energy sources, i.e., a stream that is available at a given temperature from which energy can be taken by cooling it (e.g., waste heat stream from a process). The use of the exergetic efficiency better shows the amount of power that can be recovered from the available exergy/heat source. What is more, some considerations have to be considered on the cooler. In the steam reference, the low pressure of 60 mbar imposes a condensation temperature of 36 °C at which cogeneration is hardly conceivable. However, the absence of phase change in sCO_2 allows a temperature difference in the cooler from 98 °C to 33 °C (in the preheating and cascade cycles).

Cogeneration is then still possible and would lead to outstanding exergetic efficiencies.

The four cycles present similar values of specific power output, evolving from 40 kJ/kg_{CO2} around 250 °C up to 120 kJ/kg_{CO2} near 800 °C (figure 4d). Those values are outperformed by the steam cycles presenting specific power figures up to 10 times higher. This can be explained by the evaporation phase that requires much more energy than a sensible heating process without a phase change as is the case for sCO_2 cycles. Therefore, sCO_2 cycles require a significant higher mass flow rate than steam cycles.

APPLICATION TO THE GAS TURBINE MARKET

Overview of the achievable performances

According to (Weiland et al., 2019), the penetration of the supercritical technologies into the market will mainly be motivated by its economic competitiveness. Indeed, sCO_2 cycles can be simpler and smaller and may require less components, opposed to steam cycles that require bigger economic investments (e.g., deaerator). Based on the data of 23 industrial gas turbines, an investigation towards the potential of sCO_2 cycles, to create a combined cycle configuration, has been performed. The knowledge of the exhaust temperature and mass flow is sufficient to calculate the additional power that can be delivered by the different cycle configurations thanks to the previous performance maps.

For this part of the article, cycle 20 is no longer represented as it delivers a power output very close to the preheating cycle, though requires much more components making it less cost competitive. A linear relation between the initial turbine power and the total combined cycle power that can be achieved, is represented by figure 5 and table 3. A regression with an interception defined at zero, points at a direct proportional relation (figure 5). The addition of a sCO_2 cycle adds between 33% and 48% of additional power in most of the cases (figure 6 and table 3). As expected, the total efficiency becomes higher as the efficiency of the selected bottoming cycle used is better (figure 5 and 6).

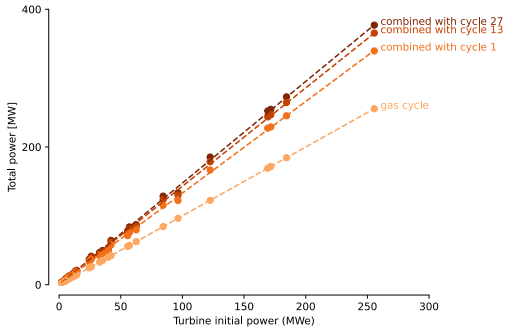

Figure 5: The linear relation between the initial gas cycle production and the total production shows that sCO_2 cycles can add up to 48% of power

Table 3: The total power production evolves linearly with the initial production of the gas cycle

Cycle	Slope	$(1-R^2)$ $\times 10^4$
Simple recuperative Brayton cycle	1.33	5.9
Preheating cycle	1.43	7.9
Dual heated and split cascade cycle	1.48	9.5

The efficiency of the open GT cycle increases with the power band of the GT. This tendency is justified by the high-end design and construction materials for the larger scale open cycle gas turbines as by the fact that the impact of inherent component losses becomes smaller as the GT size gets bigger. Improving the design of the components increases the power output and leads to a more interesting financial ROI. Therefore, the small-scale installations (<50 MWe) result in a relative higher efficiency increase when a sCO_2 cycle is integrated as a bottoming cycle. As shown on figure 6, the additional power by a closing sCO_2 cycle can reach up to 80% of the initial turbine power for the smallest installation (2 MWe).

Cost integration

Based on (Weiland et al., 2019; Wright et al., 2016), the cost of the different components can be estimated. In this preliminary study, only the capital costs of the turbine, compressor, recuperator, heater/preheater and chiller are considered. All the cost relations are taken from (Weiland et al., 2019) except the relations for the heater/preheater that are described in (Wright et al., 2016). Whereas the cost relations were established for 2017 with a CEPCI (Chemical Engineering Plant Cost Index) of 567.5, the CEPCI has been updated to 2022 value (813). The additional costs (e.g., piping, gearboxes, generators, motors) represent between 10% and 27% of the previous listed costs.

Among the different cycles, the preheating one seems the most cost competitive. Indeed, it allows a power production as high as the cycle 27 though requires much less components. A linear evolution between the additional generated power and the capital cost of the cycle is witnessed on figure 9. The cost uncertainties vary from -43% for the large-scale production hypothesis, to 50% in the single-shot assumptions. Finally, LCOE for the bottoming

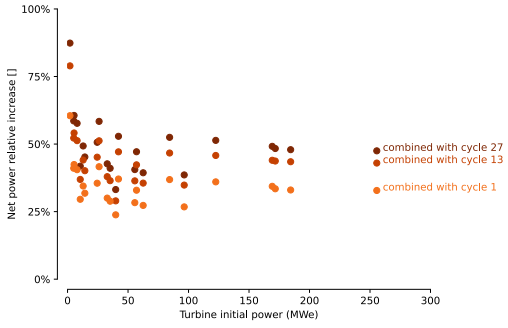

Figure 6: The relative net power increase can reach 80% for the smaller unit

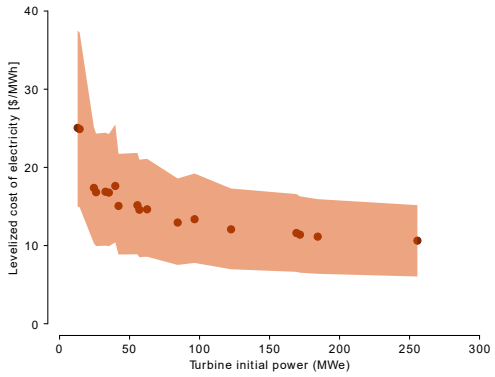

Figure 7: The LCOE of the installation is computed for 10 years, with a discount rate of 11% and an operational runtime reaching 80% of the year

sCO_2 cycle ranges between 7.6 $/MW and 38 $/MW (figure 7). and decreases with increasing installed power. For the moment, the OPEX are not integrated in the computations due to the lack of industrial experience.

ENERGY COMPARISON WITH STEAM TECHNOLOGY FOR COMMERCIAL SCALE CCGT

Most of the studies on sCO_2 are realised for a net power output under 50 MWe (Ancona et al., 2021; Gotelip et al., 2022, 2021). In order to investigate the potential of sCO_2 cycles for higher power generation in bottoming applications, a numerical comparison with an H-class CCGT from Thermoflow® has been realized. The gas cycle produces 580 MWe and a flue gas flow rate of 1037 kg/s at 670 °C; this flow goes through the HRSG. The steam combined cycle is optimised by 4-pressure levels and allows an additional power production of 280 MWe. The two cycles combined boost the efficiency up to 61% of the LHV.

In this numerical simulation, the steam cycle was replaced with sCO_2 cycles 1, 13 and 27 from the nomenclature developed in (Crespi et al., 2017). In both cases, the supercritical bottoming cycles require more power for the compression and recover less heat on the exhaust gases. Indeed, starting from 33 °C and 85 bar, the sCO_2 is compressed up to 280 bar. This compression heats the stream up to 68 °C due to the isentropic efficiency of 85%. Assuming a pinch of 30 °C, the exhaust gases cannot be

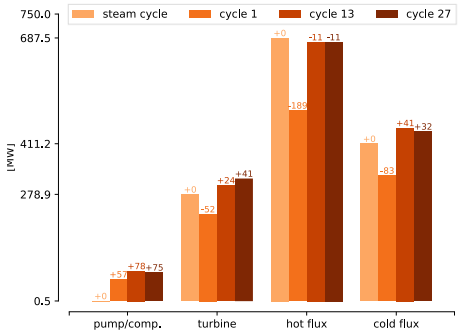

Figure 8: The supercritical cycles recover less heat and consume more power during pumping/compression

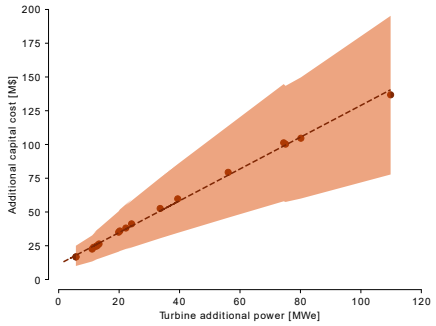

Figure 9: The capital cost of the preheating cycle evolves linearly with the additional power provided by the sCO_2 cycle ($y = 1.18x + 11.22$ with $R^2 = 0.9979$)

cooled under 98 °C. In the steam cycle, where the pumping of water is nearly isothermal, the water temperature after pumping remains low at 38 °C. On the compression aspect, the Hirn cycle remains unbeatable. For H-class CCGT bottoming cycle, finding a supercritical cycle that beats the performance of the steam bottoming one seems unbearable. The energetical comparisons of the different components on figure 8 clearly show the two main weaknesses: namely the compression/pumping stage and the hot flux recovered. Even if the supercritical turbine succeeds in delivering more power, the compression work is far higher than the pumping energy required for the water. Based on data from table 4, the cycle 27 is the most efficient and produces 8.5% less power than its steam counterpart.

As a conclusion, the performances of sCO_2 cannot compete with the current steam technology which is the product of several years of research and development. This tendency has already been evoked in (Cho et al., 2015; Huck et al., 2016; Kimzey, 2012), recalling that the lower exergy losses in the supercritical exchangers cannot balance the higher compression work required, compared to the lower pumping energy. What is more, the components are currently not yet technologically developed enough to deal with the high-power scale of an H-Class GT. As an example, the recuperators have to exchange more than 690 MW with a LMTD of approximately 10 °C. This configuration will require several heat exchangers in parallel which will have an impact on CAPEX and the complexity of the hydraulic

Table 4: The sCO_2 cycles performances remain under the steam ones, result of decades of technological innovations.

value	steam	cycle 1	cycle 13	cycle 27	unit
P_{net}	278.5	170.1	224.0	245.1	MW
ΔP_{steam}	0.0	-108.4	-54.5	-33.3	MW
η	40.6	34.1	33.1	36.2	%
ψ_{25}	75.8	46.7	60.8	67.3	%
T_{stack}	87.7	256.0	97.9	97.5	°C
Q_{cool}	411.2	328.3	452.5	443.4	MW
$T_{cool,in}$	37.4	77.5	77.5	77.5	°C
$T_{cool,out}$	37.4	33.0	33.0	33.0	°C

integration. In conclusion, sCO_2 cycles do not seem to challenge steam cycles for large power production (>100 MWe) when no cogeneration setup can be applied to validate the remaining energy from the CO_2 flow before entering the cooler.

To improve the performances of the supercritical cycles, one can work on three aspects:

1. a further technological development of the components;
2. the addition of heat recovery (implying a cogeneration setup);
3. the economic advantages.

Technology of the components

Most of the supercritical components are not available at an industrial scale and none for application in power cycles exceeding 200 MWe. The conservative hypotheses in this work assumed pinches of 30 °C for heat exchanges that involve exhaust gases, and 10 °C within the recuperators. Decreasing the pinches undoubtedly allows the cycle to be more efficient. However, the exchange area will have to be bigger, which induces more material, increasing the heat exchanger inertia and the cost related to bigger heat exchangers will be higher. With respect to the turbomachinery, the large size of the considered equipment certainly permits isentropic efficiencies up to 90% for the turbines and up to 85% for the compressors. Assuming higher efficiency values does not make sense, and this is due to the complexity of the design (small scale, huge energy densities). For instance: the complexity of the compressor design has been highlighted by (Romei et al., 2021) because of the issues encountered at the leading edge with the two-phase region. This creates difficulties as on the one hand, one tries to cool the liquid as much as possible, to maximize the compressor yield, and on the other hand, the risk of ending up in the two-phase region will be increased.

Addition of heat recovery

The implementation of cogeneration is a very interesting way allowing to increase the fuel efficiency of the cycle. Indeed, sCO_2 is not submitted to any phase change in the cooler, opposed to steam. This temperature difference can be valorised in different ways (e.g., by means of a heat pump, a residential- or industrial heat network or for a carbon-capture unit). As shown in table 4, sCO_2 goes from 78 °C to 33 °C while the condensation of water always happens at a fixed temperature (37 °C). Furthermore, the exhaust gas temperature leaving the cycle is at least 10 °C higher than compared to the steam cycle (table 4). If the amount of heat that can be recovered in this loss fraction exceeds the difference in net production with the steam cycle, sCO_2 cycles will present a higher efficiency. This said, even the integration of the SRBC on a waste heat source can lead, in combination with a cogeneration setup, to a better fuel source efficiency compared to an electrical power only casus. Considering the small equipment sizes and potential lower future investment costs, it might lead to interesting investment case studies.

Table 5: The uncertainty range for the cost estimation in M$ fluctuates from -31% to 43%

components	cost	min	max
compressor	8.2	7.4	10.3
turbine	6.2	4.6	8.0
generator	3.1	2.5	3.8
heater	28.8	20.1	43.2
preheater	44.8	31.4	67.3
recuperator	41.5	28.6	57.2
cooler	28.4	21.3	36.3
piping	20.1	8.0	32.2
TOTAL	181.0	123.9	258.1

Economical advantage

The economic advantages of sCO_2 have been highlighted in (Weiland et al., 2019). Weiland et al. proposed a general cost correlation with a power law form (eq. -5). Based on those studies (Alfani et al., 2022; Weiland et al., 2019), the cost of the equipment can be estimated and are presented in table 5. The simulation has only been realised for the preheating cycle as this is the most cost competitive one. The CEPCI has been updated to suit 2022 values and the LCOE is computed assuming 20 years of lifetime, an 11%-discount rate, and the assumption that the plant works 90% of the year. Under those hypotheses, the LCOE equals 6.02 $/MWh with uncertainties between 4.1 $/MWh and 8.6 $/MWh.

$$C = a \times SP^b \times f_T \quad (5)$$

INTEGRATION OF AMINE-BASED CARBON CAPTURE

In the upcoming years, gas turbines will play a major role in the energy transition. Indeed, the renewable energy sources are partially intermittent and add a lot of fluctuations on the power grid. To ensure the security of supply, GTs are a perfect technology that offers flexibility to the electric generation. However, the carbon emission policy is moving towards net zero emissions for the coming decades. Among the carbon capture technologies, the amine-based one is promising but leads to a significant reduction in net power production (Rubin et al., 2012; Wilberforce et al., 2019). Previously, this article proved that sCO_2 cycles have a superior exergy efficiency. As the integration of cogeneration in sCO_2 cycles is enhanced by the absence of phase change, different ways will be checked to integrate carbon capture in supercritical cycles.

Table 6: Flue gas composition at 35% EGR

components		% vol
Nitrogen	N_2	74.9
Oxygen	O_2	5.8
Carbon dioxide	CO_2	7.2
Water	H_2O	11.2
Argon	Ar	0.9

The reference case chosen for this application comes from Thermoflow® and couples a CCGT (SGT5-9000HL with a 4-stages steam cycle) with a CC unit. A schematic representation of the CCGT coupled with a CC unit can be found on figure 10a. The gas turbine produces 570 MWe, and 1018 kg/s of exhaust gases at 677 °C that are fed to the HRSG. The net power output of the steam cycle rises to 218 MWe taking into account that a part of the LP steam is used to feed the stripper. Compared to the setup without CC, the generated steam turbine power would be 279 MWe. The penalty of CC decreases the net production of the steam cycle by 28% (61 MWe). The LP steam extracted at the turbine delivers 231 MW in the reboiler of the stripper at 120 °C. In order to decrease the CC penalty, the flue gas composition is slightly different from the previous cases as EGR is applied, and presents a higher CO_2 content as shown on table 6 (35% EGR). Different configurations are imagined recovering heat for the stripper:

1. subtract sCO_2 from the bottoming cycle;
2. add a reversed Rankine cycle on the power cycle;
3. Recover heat on the exhaust gases;
4. integrate an industrial heat pump.

Maximal potential

In order to get an upper bound of the potential production, the need in heat for the stripper of the carbon capture unit is removed at first. This gives the maximal amount of power that cannot be exceeded for each cycle (table 8). Identifying first the maximal potential allows determining the margins of power that can be "sacrificed" by sCO_2 cycles to produce heat for the stripper, while trying to remain more advantageous than the steam configurations. Those results indicate that the SRBC (cycle 1) without CC already produces less power than the steam cycle coupled with CC. For the preheating cycle (cycle 13) and the dual heated and split cascade cycle (cycle 27), the margins are respectively of 7.4 and 28.4 MWe. Coming up with more efficient sCO_2 cycle configuration already appears difficult.

Subtract sCO_2

As presented on figure 10b, sCO_2 is extracted to heat the stripper somewhere in the expansion cycle. Opposed to steam, where the latent heat is ideal for an exchange at a specific temperature (latent heat of condensation), the configuration of the sCO_2 cycle does not seem relevant for the energetic integration of a carbon capture unit with subtraction in the cycle. When sCO_2 is extracted after the turbine, the sCO_2 flow is at a temperature closer to the stripper one, than at the turbine inlet. This leads to a lower exergy destruction implying a higher power generation. As an example, in the cycle 1 configuration the reboiler can be placed either before or after the turbine. When extraction takes place after, the net production of the bottoming cycle equals 128 MWe; while before, the production equals 92 MWe. The same conclusion is obtained for the cycle configuration 13. In general, the turbine outlet is the best place to recover heat because its temperature level is the closest to the temperature of the reboiler which minimizes the exergy destruction. The sCO_2 subtraction has not been applied to the cycle 27 because this is a cascade cycle, and the remaining heat after the expansion is used to heat the second turbine flow. Removing a fraction of the heat after the first turbine would therefore penalizes the rest of the cycle, while the temperature level is not high enough after the second turbine.

Reversed Rankine cycle integration

The idea behind this setup is the reversed Rankine heat pump scheme. A fraction of the CO_2 is diverted before the cooler, and recompressed up to 280 bar (178 MWe are required for compression). Due to the compression, the sCO_2 reaches 196 °C and can then be cooled down till 130 °C while assuming a pinch of 10 °C at the reboiler. 2062 kg/s of sCO_2 are needed in order to deliver 231 MW at the stripper. After the heat exchanger, the remaining energy in the flow can be recovered in the turbine (88 MWe) taking the flow back to 85 bar at 46 °C. The net consumption of this loop equals 90 MWe and is equivalent to a COP of 2.56. Whereas this configuration has an efficiency similar to the industrial heat pump configuration, it does not require a coupling with a HP as sCO_2 is the working fluid and the double pinch of the HP (pinches at the evaporator and the condenser) can be avoided. Nevertheless, working with such large flow rates is challenging and requires more technical investigations.

Heat recovery on the exhaust gases

Another configuration recovers heat on the exhaust gases. We could for instance split the heating part of the sCO_2 into two and in between those two operations, recover the heat

Table 7: Recovering heat on the exhaust gases and on the cooler for the HP increase the net production of the best cycles (13 and 27) of 10 MW

Values	cycle 1	cycle 13	cycle 27	
$Q_{flue\ gas}$	189.7	45.7	46.3	MW
Q_{cool}	0.0	98.5	97.2	MW
P_{HP}	41.3	86.9	87.5	MW
$T_{HP,out}$	92.8	56.0	55.6	°C
COP	5.6	2.7	2.6	
P_{net}	129.3	138.2	158.6	MW

Table 8: The steam cycle combined with CC can produce more power than some of the supercritical cycles without CC

	with CC	without CC			
value	steam	cycle 1	cycle 13	cycle 27	unit
P_{net}	217.7	170.7	225.1	246.1	MWe
ΔP_{steam}	0.0	-47.0	7.4	28.4	MWe
η	33.7	34.2	33.3	36.4	%
Ψ	58.8	46.1	60.8	66.5	%
T_{stack}	125.5	263.4	98.2	97.5	°C
Q_{cool}	394.1	327.8	450.5	430.1	MW
$T_{cool,in}$	32.3	77.5	77.5	77.5	°C
$T_{cool,out}$	32.3	33.0	33.0	33.0	°C

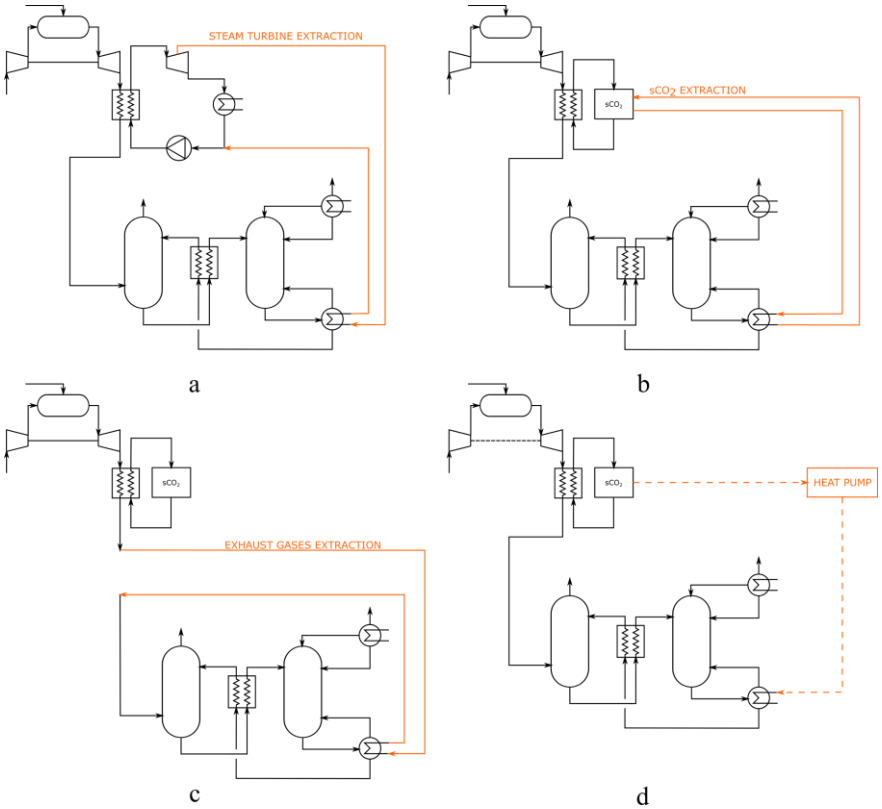

Figure 10: Cycle configuration for the integration of an amine-based carbon capture

for the reboiler (dotted exchangers in figures 2b and 2d). Due to the high recuperativeness of the supercritical cycles, there is not an issue to fit these fractioned sources into the cycle. In the preheating, the dual heated and split cascade cycles, the heat recovery has been added on the exhaust gases between the two heaters. This configuration allows to produce, respectively for the preheating (13) and cascade (27) cycles, 165 and 173 MWe.

Otherwise, in some cycles like the SRBC, the exhaust gases leave the heater at a high temperature on which energy can be extracted for different purposes. In the specific case of the cycle 1 configuration, the exhaust gases at 260 °C can be employed to feed the stripper (figure 10c). However, the available energy is insufficient to completely heat the stripper. Given a pinch of 30 °C, only 60% of the heat needed can be extracted from the exhaust gases. This solution is not applicable to the most efficient cycle configurations (cycles 13 and 27) because the flue gas temperature at stack level is too low (respectively 98.2 °C and. 97.5 °C).

Table 9: The integration of a heat pump on the cooler decreases the power production by approximately 100 MWe

values	cycle 1	cycle 13	cycle 27	
$T_{HP,in}$	77.5	77.5	77.5	°C
$T_{HP,out}$	45.5	50.2	49.5	°C
COP	2.20	2.39	2.35	
P_{HP}	105.2	96.8	98.1	MW
Q_{HP}	125.8	134.2	132.9	MW

Industrial heat pump on the cooler

In the cooler, sCO_2 is cooled from 78 °C ($T_{HP,in}$) till 33 °C. The reboiler of the striper requires a temperature of 120 °C. As shown on figure 10d, an industrial heat pump (set up including MVR) can realise this heat transfer. Depending on the technology, between 330 MW and 450 MW are released at the CO_2 cooler (Q_{cool}) and can be used as a heat source. Industrial heat pumps of this size and temperature levels (120 °C) exist (Armstrong International, 2023), though not within this power range. For a heat sink at 120 °C, the COP can be approximated by a quadratic law (eq. -6) of the final heat source temperature (Armstrong International, 2023). Due to the high fluctuations of the properties of sCO_2, near its critical point, the evolution of the temperature along the isobaric curve decreases the heat exchanger efficiency. Taking into account the specific heat of sCO_2, the final hot source temperature ($T_{HP,out}$) leaves the heat pump between 45 °C and 50 °C, allowing COPs between 2.2 and 2.4. This decreases the power production by roughly 100 MWe due to the consumption of the HP (P_{HP}), as shown on table 7.

Industrial heat pump on both the cooler and the exhaust gases

In an energetically updated (though more capital intensive) configuration, the industrial heat pump will recover heat from the CO_2 stream (Q_{cool} from $T_{cool,in}$ to $T_{HP,out}$) and the

exhaust gases ($Q_{flue\ gas}$ from T_{stack} to $T_{HP,out}$). This allows to increase the final source stream temperature of the HP ($T_{HP,out}$) and thus improve the COP of the installation. When heat is recovered on both flows, the thermodynamical optimum is obtained when both source streams reach the same final temperature $T_{HP,out}$. As shown on table 7, improved COPs are expected for cycle configurations 13 and 27. In the cycle 1 configuration, the high temperature of the exhaust gases T_{stack} boosts the COP up to 5.6 and the amount of energy available on the exhaust gases is sufficient enough so that no heat has to be taken from the cooler.

$$COP = 7.50 \times 10^{-4} T^2 - 3.21 \times 10^{-2} T + 2.11 \quad (6)$$

Comparisons

A comparison between the different configurations that have been presented before can be found on table 10. It can be observed that the addition of heat recovery on the exhaust gases at the location that minimises the exergy destruction within the cycle, is the most interesting one. Indeed, the net generated power decrease is minimal and no investment in HP technology is required. On the other hand, direct heat exchange by the amine flow in the flue gas heat exchanger might entail risks due to local hot spots that could degrade the amines. The risk of amine destruction is a general risk that can be addressed when sCO_2 will be used as one works on sensible heat transfer instead of latent heat transfer. Compared to the sCO_2 subtract and the inverted Rankine cycle layout, as CO_2 is used as the heat transfer fluid, the hydraulic CO_2 network becomes bigger which enlarges the scope of the CO_2 leakage management. Though easy for the SRBC and the preheating cycle, the integration of the subtraction becomes complex for the cascaded cycle. Due to the constant condensation temperature of steam; the use of steam at the reboiler is a very interesting option and the performances of the initial steam configuration will be difficult to beat (if not unbeatable). Nevertheless, with the assumption that the remaining heat in the exhaust gases is recovered to 70 °C (heat network), the fuel utilisation ratios of the cycle 13 and 27 differ by 0.1% from the bottoming cycle casus (54.5%).

CONCLUSION

Within this paper, we extended our knowledge on sCO_2 cycles with performance maps that allow to characterise four promising cycles for heat to power conversion. For a range of temperatures between 200 °C and 800 °C we now dispose of curves that determine the recoverable power for a source at a given temperature. The sCO_2 cycle provide efficiencies closed to the Hirn cycle though the smaller equipment, potential simpler cycle configurations and reduced costs offer clear advantages. Indeed, the application as a bottoming cycle for small-scale gas turbine (<50 MWe) is relevant and leads to LCOE between 6 $/MWe and 38 $/MWe. While looking at larger scale production (280 MWe), one can observe that the performance of the steam cycle is hardly beatable. This can be explained by the associated compression work for the sCO_2 cycle (compared to the neglectable pumping work for the steam Rankine cycle). Nevertheless, the absence of a phase change allows heat to be recovered on the supercritical cooler for cogeneration. We therefore studied how an amine-based carbon capture unit could be integrated on a CCGT where the steam cycle is replaced by a sCO_2 cycle. Here again, the best performances are found when heat is recovered directly on the exhaust gases at the temperature level that minimizes the exergy destruction.

ACKNOWLEDGEMENTS

We would like to warmly thank Baker Hughes, Heatric and Siemens Energy for the interest they have shown in this study. Their industrial point of view adds value to this paper by orienting the research to the most likely trends.

REFERENCES

Ahn, Y., Bae, S.J., Kim, M., Cho, S.K., Baik, S., Lee, J.I., Cha, J.E., 2015. Review of supercritical CO2 power cycle technology and current status of research and development. Nuclear engineering and technology 47, 647–661.

Alfani, D., Astolfi, M., Silva, P., Persico, G., 2022. Technical report: Off design performance of the sCO2 power unit connected to the cement plant heat recovery, Supercritical CO2 power cycles demonstration in Operational environment Locally valorising industrial Waste Heat.

Alfani, D., Binotti, M., Macchi, E., Silva, P., Astolfi, M., 2021. sCO2 power plants for waste heat recovery: design optimization and part-load operation strategies. Applied Thermal Engineering 195, 117013.

Ancona, M.A., Bianchi, M., Branchini, L., De Pascale, A., Melino, F., Peretto, A., Torricelli, N., 2021. Systematic comparison of ORC and s-CO2 combined heat and power plants for energy harvesting in industrial gas turbines. Energies 14, 3402.

Armstrong International, 2023. Pompes à chaleur industrielles haute température [WWW Document]. Armstrong | EMEA. URL https://armstronginternational.eu/fr/produits/solutions-premontees-de-pompe-a-chaleur/ (accessed 3.17.23).

Baggiani, M., Bruttini, P., Cagnac, A., De Vos, Y., Glos, S., Persico, G., Spolcova, J., Le Pierres, R., Messina, G., Tassou, S., 2022. Supporting document for the CO2OLHEAT technical poster presented during the Supercritical CO2 Power Cycles Symposium (21 Feb – 24 Feb 2022, San Antonio, Texas, USA) 12.

Biondi, M., 2020. Business case for sCO2 Waste Heat Recovery System.

Brun, K., Friedman, P., Dennis, R. (Eds.), 2017. Fundamentals and applications of supercritical carbon

dioxide (sCO2) based power cycles, Woodhead Publishing series in energy. Elsevier, Woodhead Publishing, Oxford.

Cagnac, A., Mecheri, M., Bedogni, S., 2019. Configuration of a flexible and efficient sCO2 cycle for fossil power plant, in: 3rd European Supercritical CO2 Conference. pp. 19–20.

Cho, S.K., Kim, M., Baik, S., Ahn, Y., Lee, J.I., 2015. Investigation of the bottoming cycle for high efficiency combined cycle gas turbine system with supercritical carbon dioxide power cycle, in: Turbo Expo: Power for Land, Sea, and Air. American Society of Mechanical Engineers, p. V009T36A011.

Crespi, F., Gavagnin, G., Sánchez, D., Martínez, G.S., 2017. Supercritical carbon dioxide cycles for power generation: A review. Applied Energy 195, 152–183.

Dincer, I., Rosen, M.A., 2012. Exergy: energy, environment and sustainable development. Newnes.

Gotelip, T., Gampe, U., Glos, S., 2022. Optimization strategies of different SCO2 architectures for gas turbine bottoming cycle applications. Energy 250, 123734.

Gotelip, T., Gampe, U., Glos, S., 2021. Techno-economic optimization method and its application to an sCO2 gas turbine bottoming cycle, in: 4th European SCO2 Conference 2021.

Huck, P., Freund, S., Lehar, M., Peter, M., 2016. Performance comparison of supercritical CO2 versus steam bottoming cycles for gas turbine combined cycle applications, in: 5th International Supercritical CO2 Power Cycle Symposium.

Kimzey, G., 2012. Development of a Brayton bottoming cycle using supercritical carbon dioxide as the working fluid. Electric Power Research Institute, University Turbine Systems Research Program, Gas Turbine Industrial Fellowship, Palo Alto, CA.

Lemmon, E.W., Bell, I.H., Huber, M.L., McLinden, M.O., 2018. NIST Standard Reference Database 23: Reference Fluid Thermodynamic and Transport Properties-REFPROP, Version 10.0, National Institute of Standards and Technology.

Liu, Y., Wang, Y., Huang, D., 2019. Supercritical CO2 Brayton cycle: A state-of-the-art review. Energy 189, 115900.

Romei, A., Gaetani, P., Persico, G.B.A., others, 2021. Design and off-design analysis of a highly loaded centrifugal compressor for sCO2 applications operating in near-critical conditions, in: 4th European SCO2 Conference for Energy Systems. pp. 1–10.

Rubin, E.S., Mantripragada, H., Marks, A., Versteeg, P., Kitchin, J., 2012. The outlook for improved carbon capture technology. Progress in energy and combustion science 38, 630–671.

Span, R., Wagner, W., 1996. A New Equation of State for Carbon Dioxide Covering the Fluid Region from the Triple-Point Temperature to 1100 K at Pressures up to 800 MPa. Journal of Physical and Chemical Reference Data 25, 1509–1596.

Stepanek, J., Entler, S., Syblik, J., Vesely, L., Dostal, V., Zacha, P., 2020. Parametric study of S-CO2 cycles for the DEMO fusion reactor. Fusion Engineering and Design 160, 111992.

Weiland, N.T., Lance, B.W., Pidaparti, S.R., 2019. SCO2 power cycle component cost correlations from DOE data spanning multiple scales and applications, in: Turbo Expo: Power for Land, Sea, and Air. American Society of Mechanical Engineers, p. V009T38A008.

White, C.W., Weiland, N.T., 2018. Evaluation of Property Methods for Modeling Direct-Supercritical CO2 Power Cycles. Journal of Engineering for Gas Turbines and Power 140, 011701.

White, M.T., Bianchi, G., Chai, L., Tassou, S.A., Sayma, A.I., 2021. Review of supercritical CO2 technologies and systems for power generation. Applied Thermal Engineering 185, 116447.

Wilberforce, T., Baroutaji, A., Soudan, B., Al-Alami, A.H., Olabi, A.G., 2019. Outlook of carbon capture technology and challenges. Science of the total environment 657, 56–72.

Wright, S.A., Davidson, C.S., Scammell, W.O., 2016. Thermo-economic analysis of four sCO2 waste heat recovery power systems, in: Fifth International SCO2 Symposium, San Antonio, TX, Mar. pp. 28–31.

Zhao, Q., Mecheri, M., Neveux, T., Privat, R., Jaubert, J.-N., 2016. Thermodynamic model investigation for supercritical CO2 Brayton cycle for coal-fired power plant application, in: Proceedings of the Fifth International Supercritical CO2 Power Cycles Symposium, San Antonio, TX, USA. pp. 29–31.